Medicinal Chemistry Research (2019) 28:1783–1795
https://doi.org/10.1007/s00044-019-02415-4

MEDICINAL CHEMISTRY RESEARCH

ORIGINAL ARTICLE

Synthesis, sciatic nerve block activity evaluation and molecular docking of fluoro-substituted lidocaine analogs as local anesthetic agents

Wen Li[1,2,3] · Ying Yan[1] · Yingjie Chang[1] · Lina Ding[1,3] · Hongmin Liu[1,3] · Qidong You[2]

Received: 1 January 2019 / Accepted: 26 July 2019 / Published online: 5 August 2019

Abstract

Thirty fluoro-substituted lidocaine analogs (**10a–e**, **11a–e**, **14a–e**, **15a–e**, **18a–e** and **19a–e)** were synthesized, and their sciatic nerve block activity were evaluated as local anesthesia. Most of the compounds displayed significant potency, and compound **10a** in particular was much more potent than the parent lidocaine. Fifteen analogs including **10a** demonstrated pKa values of 7.5–7.8 suitable for local anesthesia. Compound **10a**, **14e**, and lidocaine were docked into three target receptors of local anesthetics by molecular docking studies to delineate structure-activity relationships and explain the differences in activities. Hydrophobic interactions and hydrogen bonds were identified key to molecular binding, suggesting that optimization of these interactions and/or trifluoro-substitution at the benzene ring of lidocaine could enhance the properties of lidocine analogs for local anesthesia.

Keywords Lidocaine · Synthesis · Local anesthetic activity · Molecular docking

Introduction

Lidocaine (Fig. 1), also named as lignocaine and xylocaine, is a well-known local anesthetic (Li et al. 2018; E Silva et al. 2018) and a broad-spectrum antiarrhythmia (Hebbes and Thompson 2018; McLeod et al. 2017), has been used in clinical practice for more than 60 years. Recently, lidocaine become in the spotlight again for its new diversity activities has been discovered, such as reduced risk of tumor metastasis and recurrence (D'Agostino et al. 2018; Le Gac et al. 2017; Tavare et al. 2012; Wang et al. 2016), antimicrobial effect (Adler et al. 2017; Epstein 1998; Estebe 2017; Neuwersch et al. 2017; Tulgar et al. 2018), anti-inflammatory effect (Kan et al. 2018; Wang et al. 2018), anti-acute lung injury effect (Bonniaud, Camus 2015; Van Ness et al. 2013), and reduced the cognitive impairment (Lin et al. 2012; Yang et al. 2017). These imply that we still have much to learn about the structure and activity relationships (SAR) of lidocaine and its analogous.

The voltage-gated sodium channel (VGSC) has been found to be the target for local anesthetics (Boukhabza et al. 2016; Wang et al. 2015), gamma aminobutyric acid receptor (GABAA-R) (Nakahata et al. 2010; Sugimoto et al. 2000; Ye et al. 1999) and N-methyl-D-aspartate acid receptor (NMDA-R) (Chen et al. 2011; Gronwald et al. 2012; Zhang et al. 2014) are also targets for some local anesthetics. Therefore, lidocaine may be a multi-target agent and comprehensive research into the relationships between ligands and multiple targets may be useful for the rational design of local anesthetic agents.

Structural modifications of lidocaine have been previously explored on replacing the CH_3 group on the phenyl ring or the CH_2CH_3 group on the amine with different alkyl

✉ Wen Li
liwen@zzu.edu.cn

✉ Qidong You
youqd@gmail.com

1 School of Pharmaceutical Sciences, Zhengzhou University, 450002 Zhengzhou, PR China

2 Jiangsu Key Laboratory of Drug Design and Optimization and Department of Medicinal Chemistry, China Pharmaceutical University, 210009 Nanjing, PR China

3 Collaborative Innovation Center of New Drug Research and Safety Evaluation, Henan Province & Key Laboratory of Technology of Drug Preparation (Zhengzhou University), Ministry of Education & Key Laboratory of Henan Province for Drug Quality and Evaluation, 450002 Zhengzhou, PR China

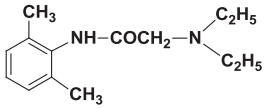

Fig. 1 Structure of lidocaine

groups (Strother et al. 1977). Meanwhile, our group has reported sodium channel blockers containing benzene rings substituted with fluorine or trifluorine in the *o*-, *m*- and *p*-positions, such as substituted imipramine compounds (Li et al. 2010; Li and You 2007) and fluoro-ropivacaine analogs (Li et al. 2017). Some of these compounds exhibited greater potency than the parent compounds when tested for infiltration anesthesia, surface anesthesia and analgesic actions. In addition, when the phenyl ring was substituted with fluorine at position-1, imipramine exhibited substantially increased antidepressant activity and significantly decreased anticholinergic toxicity (Kyburz and Spiegelberg 1975). In fact, fluoro-substituted drugs account for a considerable proportion of clinical treatment drugs, and the total number has exceeded 180 (Wang and Liu 2011). The fluorine substitution strategy in drug design is also one of the important research strategies for drug structural transformation (Ojima 2004). These exciting findings inspired us to further research fluoro-substituted sodium channel blockers.

Herein we presented the syntheses of new fluoro-substituted lidocaine analogs, the evaluation of their sciatic nerve block activities, and the potential mechanism of action based on molecular docking, as well as their dissociation constants (pKa).

Results and discussion

Synthesis

The synthesis route of the lidocaine analogs followed the general pathway outlined in Scheme 1. Firstly, 2-Trifluoromethyl aniline (**1**) was converted to sulfilimine (**2**), and then treated with succinimide to form 2-trifluoromethyl-6-[(methylthio)methyl]aniline (**3**). Treatment of compound **3** with $NaIO_4$ produced 2-trifluoromethylphenyl-6-(methylsulfoxidemethyl)aniline (**4**), which was subsequently treated with dry hydrogen chloride gas to afford compound (**5**). Catalytic hydrogenation of **5** using 10% Pd–C gave a 3:1 mixture of 2-trifluoromethyl-6-methylaniline (**6**) and 2-trifluoromethyl-6-(methoxymethyl) aniline (**7**). After chloroacylation and N-alkylation reactions on intermediates **3**, **6**, and **7**, 30 lidocaine analogs were obtained.

Biology

All of the synthesized compounds were tested in vitro for their sciatic nerve block activities in toads, using lidocaine hydrochloride as a positive control. The ED_{50} (mg/mL) and the latent period time (min) were determined according to previously described methods (Li et al. 2017). The biological activities are summarized in Table 1.

The ED_{50} of all compounds were in the range of 0.010–0.140 mg/mL except compound **19e** which demonstrated no sciatic nerve block activity. Under the same conditions, the ED_{50} of the reference compound lidocaine was 0.019 mg/mL. Six compounds, namely **10a**, **11a**, **11d**, **15a**, **15c,** and **19a**, were much potent with ED_{50} in the range of 0.010–0.019 mg/mL. Compound **10a** in particular displayed the highest block activity, which was almost twice that of lidocaine. Although compounds **11c**, **14c**, **14d**, **15d**, **18b**, and **18c** were slightly weaker than lidocaine, they also exhibited significant potency of 0.020–0.023 mg/mL. Compounds **10b**, **10c**, **10d**, **11b**, **14a**, **14b**, **15b**, **18a**, **18d**, **19b**, **19c**, and **19d** showed moderate potency of 0.028–0.054 mg/mL, while the least potent compounds **10e**, **11e**, **14e**, **15e**, **18e**, and **19e** gave ED_{50} greater than 0.086 mg/mL. Structurally, the morpholinyl group was obviously not favorable for nerve block activity.

The latent periods of the analogs were 18.0–50.7 min while that of lidocaine was 37.2 min. Among of these compounds, only **11a**, **18b**, **18c**, **18d**, and **19a** showed longer latent periods than lidocaine. Structurally, the propyl on the amino and the methyl on the phenyl group may be the reason why the latent periods of the compounds have been extended.

Dissociation constant

pKa (dissociation constant) is an important physicochemical parameter for local anesthetics. Most local anesthetics have pKa values between 7.0 and 7.7. When a drug has pKa below 7.0, it is not sufficiently ionized at physiological pH to produce any anesthetic effect, even though it can penetrate the cell membrane. In contrast, when a drug has pKa above 9.5, it is almost fully ionized at physiological pH and has difficulty penetrating the axon, thus limiting its effectiveness. The pKa values of the lidocaine analogs in this study were determined using the potentiometric titration method (Li et al. 2017). The volume of hydrochloric acid added was plotted against the pH of the solution.

Dissociation constants were obtained as the pH value at the half-equivalence point of the titration curve. The pKa values of the lidocaine analogs are summarized in Table 1. Among all the compounds, **10a**, **10b**, **10c**, **11a**, **11b**, **11c**, **14a**, **14b**, **14c**, **15a**, **15b**, **15c**, **18a**, **18c,** and **19c** showed

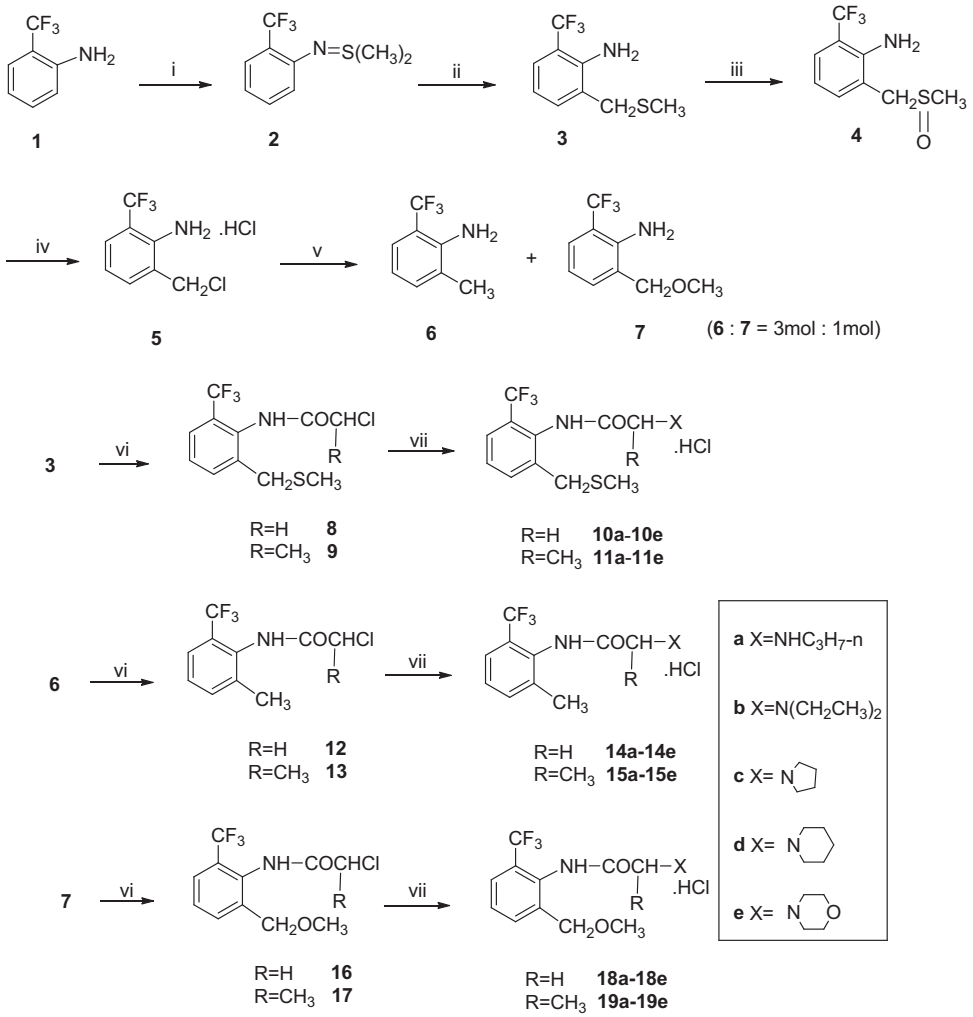

Scheme 1 Synthesis procedure for compounds **10a–e**, **11a–e**, **14a–e**, **15a–e**, **18a–e**, and **19a–e**. Reagents and conditions: (i) (1) P_2O_5, DMSO, r. t., 8 h; (ii) Succinimide, CH_2ClCH_2Cl, reflux, 4 h; (iii) $NaIO_4$, CH_3OH, r. t., 4 h; (iv) HCl, CH_2ClCH_2Cl, 50 °C., 1 h; (v) 10% Pd–C, $HCOONH_4$, CH_3OH, r. t., 0.5 h; (vi) $ClCH_2COCl$ or $ClCH(CH_3)COCl$, CH_3COOH–CH_3COONa, r. t., 0.5 h; (vii) (1) HX, K_2CO_3, 80 °C, 10 h; (2) HCl

pKa values of 7.5–7.8 appropriate for local anesthetics. The others displayed pKa values below 7.5, suggesting that they would remain in the uncharged form at the pH of body fluids.

Docking studies

Molecular docking studies

To investigate the potential mechanism of local anesthetics, three representative compounds of different levels activity, namely compound **10a** (strongest activity, 0.010 mg/mL), **14e** (lowest activity, 0.14 mg/mL), and lidocaine (0.019 mg/mL), were selected as subjects for molecular docking studies, and researched their binding models with three different potential targets of local anesthetics (VGSC, GABAA-R, and NMDA-R).

One molecular target of local anesthetics is the human VGSC and previous studies have identified that the active site is the cavity consisting of the I-S6 to IV-S6 segments (Boukhabza et al. 2016; Lipkind, Fozzard 2010). The first crystal structure of human VGSC Nav1.4 has been revealed by the Yan Ning's research group. The structure is complex with its specific regulatory subunit β_1 and has a resolution of 3.2 Å (PDB code: 6AGF) (Pan et al. 2018). This could provide a reliable template for further understanding of the potential mechanism of local anesthesia. We therefore selected 6AGF as the receptor for our docking studies.

The GABAA-R is an another potential target of local anesthetics (Amin and Subbarayan 2017; Sugimoto et al. 2000). Chen et al. have established two crystal structures of human GABAA-R (PDB code: 6D1S and 6CDU) and revealed the possible binding sites for endogenous neurotransmitter GABA and anesthetics (Chen et al. 2018). In this study, 6D1S was selected as the docking receptor because it offered a higher resolution (3.2 Å) than 6CDU (3.45 Å).

The NMDA-R is important for controlling synaptic plasticity and memory function, and could be another potential target of local anesthetics (Zhang et al. 2014). In

Table 1 The infiltration anesthesia activities of compounds **4b**, **4c**, **4j**, and **4l**

Compound	The regress equation of AP decreasing extent(%) and compounds concentration	ED_{50} (mg/mL)	The regress equation of Latent period (min) and compounds concentration	Latent period (min)	pKa
10a	$y = 72.75\log x + 195.5$	0.010	$y = -26.97\log x - 24.34$	29.6	7.6
10b	$y = 96.61\log x + 186.12$	0.039	$y = -27.45\log x - 9.28$	29.4	7.5
10c	$y = 110.43\log x + 216.60$	0.031	$y = -25.81\log x - 14.74$	24.2	7.7
10d	$y = 105.33\log x + 202.06$	0.036	$y = -25.93\log x - 13.64$	23.8	6.8
10e	$y = 109.57\log x + 150.89$	0.120	$y = -36.67\log x - 7.57$	26.2	5.5
11a	$y = 89.49\log x + 218.70$	0.013	$y = -26.85\log x - 8.43$	42.2	7.7
11b	$y = 102.71\log x + 192.48$	0.041	$y = -20.25\log x - 4.19$	23.9	7.6
11c	$y = 93.21\log x + 206.39$	0.021	$y = -19.13\log x - 2.80$	29.3	7.5
11d	$y = 98.32\log x + 219.23$	0.019	$y = -39.65\log x - 36.45$	31.8	7.3
11e	$y = 142.27\log x + 199.47$	0.089	$y = -31.38\log x - 4.57$	28.4	6.1
14a	$y = 92.43\log x + 168.68$	0.052	$y = -33.08\log x - 9.97$	32.5	7.5
14b	$y = 93.16\log x + 188.02$	0.033	$y = -9.20\log x + 4.37$	18.0	7.5
14c	$y = 78.71\log x + 178.95$	0.023	$y = -16.66\log x - 3.49$	23.8	7.6
14d	$y = 75.85\log x + 175.73$	0.022	$y = -16.02\log x - 1.75$	24.8	7.1
14e	$y = 124.57\log x + 156.37$	0.140	$y = -29.21\log x + 7.86$	32.8	6.0
15a	$y = 63.12\log x + 165.13$	0.015	$y = -17.32\log x - 5.29$	26.3	7.7
15b	$y = 102.36\log x + 183.17$	0.050	$y = -32.81\log x - 16.99$	25.7	7.5
15c	$y = 125.95\log x + 269.75$	0.018	$y = -34.00\log x - 28.82$	30.5	7.8
15d	$y = 115.22\log x + 234.59$	0.025	$y = -32.11\log x - 21.54$	29.9	7.3
15e	$y = 116.76\log x + 175.00$	0.085	$y = -35.14\log x - 8.32$	29.3	6.2
18a	$y = 97.13\log x + 187.95$	0.038	$y = -27.32\log x - 3.40$	35.4	7.5
18b	$y = 110.37\log x + 232.95$	0.022	$y = -14.93\log x + 14.25$	39.0	7.4
18c	$y = 92.45\log x + 205.11$	0.021	$y = -29.44\log x - 11.69$	37.7	7.5
18d	$y = 104.09\log x + 183.65$	0.052	$y = -41.33\log x - 10.07$	43.0	7.3
18e	$y = 116.31\log x + 171.63$	0.090	$y = -28.82\log x - 5.14$	25.0	6.0
19a	$y = 63.21\log x + 160.28$	0.018	$y = -41.89\log x - 22.39$	50.7	7.3
19b	$y = 102.93\log x + 208.27$	0.029	$y = -23.97\log x - 11.96$	24.9	7.3
19c	$y = 129.74\log x + 243.94$	0.032	$y = -32.66\log x - 19.52$	29.3	7.5
19d	$y = 117.13\log x + 217.71$	0.037	$y = -18.89\log x - 5.85$	21.2	7.1
19e	No activity	–	–	–	6.0
lidocaine	$y = 111.39\log x + 241.73$	0.019	$y = -27.64\log x - 10.38$	37.2	7.9

the RCSB protein database bank, there are 20 X-ray crystal structures of the human NMDA-R, among which 5I2N (Volgraf et al. 2016) gives a relatively high resolution and its ligand is similar in structure to our compounds. Therefore, 5I2N was selected as the docking receptor in our studies.

VGSC docking

Compounds **10a**, **14e,** and lidocaine were docked into the predicted binding site of VGSC and the results showed that compound **10a** had the best score (−6.2737), followed by lidocaine (−5.9143) and **14e** (−5.7564). When compound **10a**, **14e**, and lidocaine were placed in the center of the channel lumen, the substituted benzenes of compounds **10a**, **14e,** and lidocaine were found to occupy the hydrophobic cavity surrounded by residues Phe-436, Phe-1601, Leu-443, Tyr-450, Phe-797, forming π-π stacking interactions with the residue Phe-1601 (Fig. 2). The differences in potency of these compounds could be explained by that the trifluoromethyl and dimethylsulfide groups of **10a** had stronger hydrophobic interactions with the surrounding residues Tyr-1593, Phe-1586, Phe-1290, and Phe-797 than the substituted groups of lidocaine (Fig. 2a, c). Therefore, Compound **10a** bound tighter to the active site than lidocaine and was more potent. Conversely, the hydrophilic morpholine group of compound **14e** showed weaker affinity to the surrounding hydrophobic residues Phe-1586, Phe-1290, Tyr-1593, and Phe-797 (Fig. 2b); hence lower potency than **10a** and lidocaine. We herein propose that the ligand activity may be enhanced by increasing the hydrophobicity of the substituents appropriately.

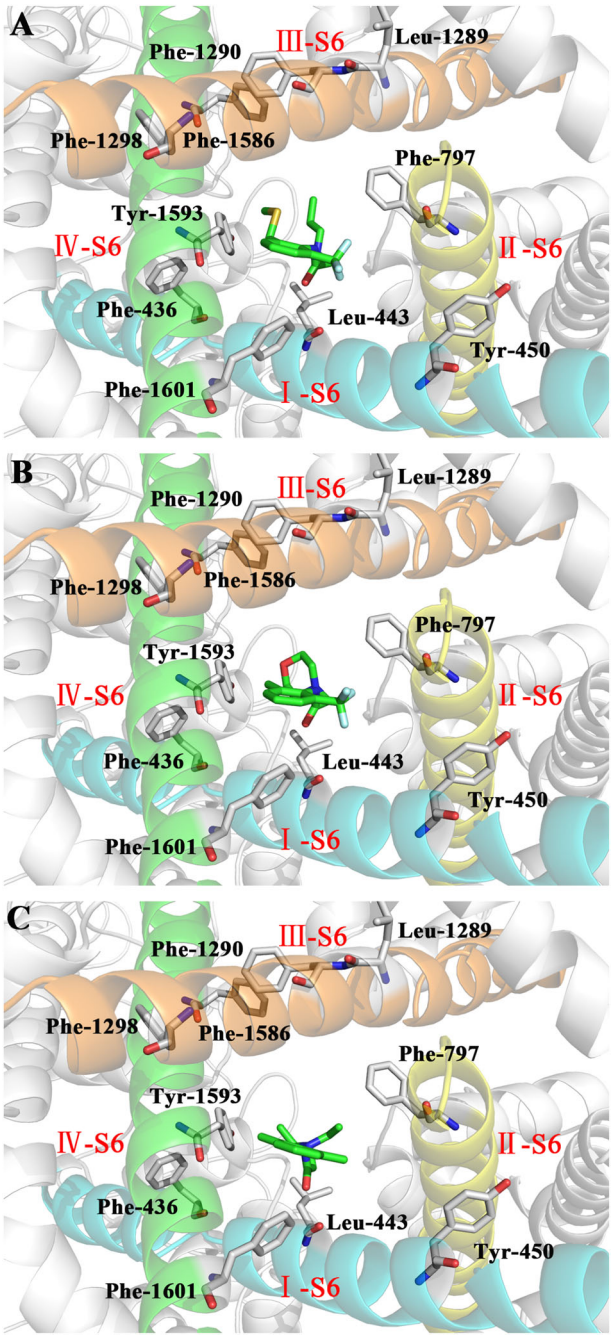

Fig. 2 Binding models of compound **10a** (**a**), **14e** (**b**) and lidocaine **c** in the active site of VGSC. Ligands were shown in green stick modes, and key residues of VGSC were shown in white stick models. The nitrogen, oxygen, fluorine and sulfur atoms were shown in blue, red, cyan and yellow, respectively. I-S6 to IV-S6 segments of VGSC were shown in cyan, yellow, orange and green cartoon ribbons, respectively (Color figure online)

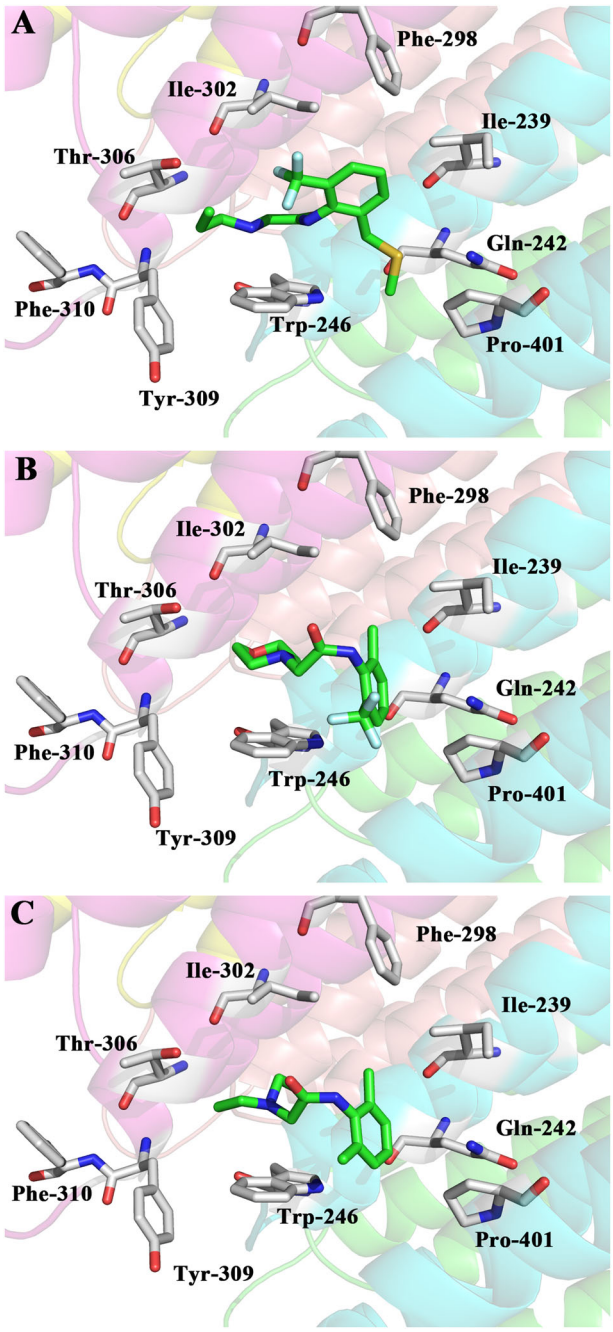

Fig. 3 Binding models of compound **10a** (**a**), **14e** (**b**), and lidocaine **c** in anesthetics binding site of GABAA-R. Ligands were shown in green sticks, and key residues of GABAA-R were shown in white stick models. The nitrogen, oxygen, sulfur, and fluorine atoms were shown in blue, red, yellow and cyan, respectively (Color figure online)

GABAA-R docking

Compounds **10a**, **14e**, and lidocaine were docked into the binding site of GABAA-R (Fig. 3), revealing the docking score of **10a**, **14e**, and lidocaine as −5.8481, −5.4714, −5.7675, respectively. The benzene groups of **10a**, **14e**, and lidocaine formed hydrophobic interactions with surrounding residues Ile-302, Phe-298, Ile-239, Gln-242, Pro-401, and Trp-246. Apart from these hydrophobic interactions, the trifluoromethyl and dimethylsulfide groups of **10a** had stronger hydrophobic interactions with the surrounding residues than those of the methyl groups of lidocaine, and

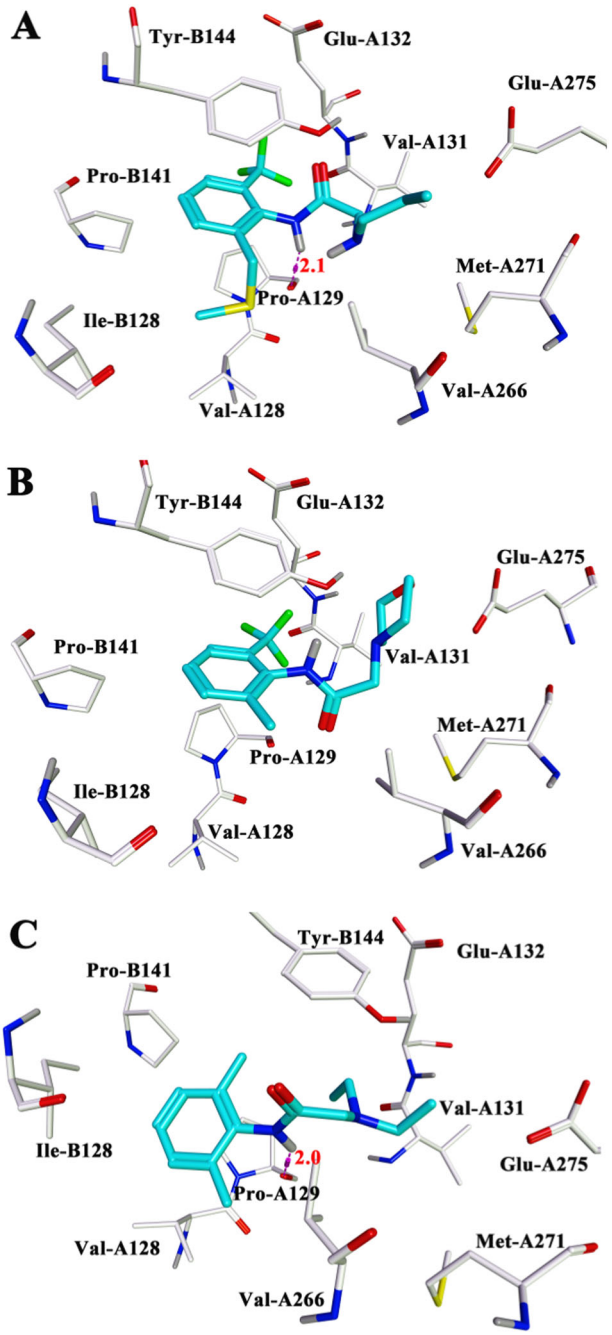

Fig. 4 Binding models of compound **10a** (**a**), **14e** (**b**), and lidocaine **c** in the active site of NMDA-R. Ligands were shown in cyan stick models, and key residues of NMDA-R were shown in white stick models. The nitrogen, oxygen, hydrogen, fluorine and sulfur atoms were shown in blue, red, gray, green and yellow, respectively. And the corresponding distances were given in Å (Color figure online)

the substituted benzene of compound **10a** could also form π–π stacking interactions with the residue Phe-298 (Fig. 3a, c). Thus, compound **10a** demonstrated a stronger local anesthetic effect than lidocaine because of the tighter binding. Compared with the propylamino group of compound **10a** and the diethylamino group of lidocaine, the substituted morpholine of **14e** afforded weak hydrophobic interactions with surrounding residues Ile-302, Phe-310, Tyr-309, and Trp-246, hence the lowest potency among the three compounds (Fig. 3b). These results again indicate that hydrophobic interactions are crucial to activity.

NMDA-R docking

Compounds **10a**, **14e**, and lidocaine were docked well into the binding site of NMDA-R and a similar docking pattern was obtained with docking score of −6.8702, −6.0990, and −6.7101, respectively (Fig. 4). The benzene groups of compounds **10a**, **14e**, and lidocaine formed hydrophobic interactions with surrounding residues Val-A128, Pro-A129, Ile-B128, Pro-B141, and Tyr-B144. The amide groups of **10a** and lidocaine formed hydrogen bonds with Pro-A129 at distances of 2.1 Å (N–H···O = Pro-A129) and 2.0 Å (N–H···O = Pro-A129), respectively. Meanwhile, both the propylamino group of **10a** and the diethylamino group of lidocaine formed hydrophobic interactions with residues Val-A266, Met-A271, and Val-A131. Despite all these interactions, the higher potency of **10a** was likely explained by the stronger hydrophobic interactions formed by the trifluoromethyl and dimethylsulfide groups on the benzene ring of **10a**, with the surrounding residues Val-A128, Pro-A129, Ile-B128, Pro-B141 and Tyr-B144, than those by the methyl groups on benzene ring of lidocaine (Fig. 4a, c). Moreover, the substituted benzene of **10a** also formed π–π staking interactions with Tyr-B144. In contrast, no hydrogen bond formation was observed between **14e** and NMDA-R, and the hydrophobicity of the substituted morpholine in **14e** was poor (Fig. 4b), resulting in loose binding and hence low potency. Therefore, it was speculated that hydrogen bonds and hydrophobic interactions could enhance the binding of the compounds to NMDA-R.

Experimental

(2-Trifluoromethyl)-6-[(methylthio)methyl]aniline (3)

2-TriFluoromethyl aniline **1** (100 mL, 0.8 mol) and phosphorus pentoxide (340 g, 2.4 mol) were suspended in 1600 mL CH_2Cl_2 and stirred at room temperature while DMSO (400 mL, 5.6 mol) and triethylamine (78 mL, 0.56 mol) were added slowly during 30 min, the reaction mixture was heated to 30 °C for 8 h. Then, the reaction mixture was poured to 200 mL 10% ice NaOH solution. N-(2-trifluoromethylphenyl)-S, S-dimethyl sulfilimine (**2**, 104.0 g) was obtained by separated CH_2Cl_2 layer, dried with anhydrous sodium sulfate and removed solvent by rotaryevaporation. Compound **2** (104 g, 0.47 mol) and

succinimide (2.3 g, 0.023 mol) were then added to 600 mL 1, 2-dichloroethane, the mixture was heated to reflux for 4 h. The reaction mixture was poured to 200 mL 10% ice NaOH solution. 2-Trifluoromethyl-6-[(methylthio)methyl] aniline (**3**, 80 g) was obtained by separated 1,2-dichloroethane layer, dried with anhydrous sodium sulfate and removed solvent by rotaryevaporation. Yield 77%.

(2-Trifluoromethylphenyl)-6-[(methylthio) methyl] aniline (4)

At 0 °C, $NaIO_4$ (4.8 g, 0.023 mol) was dissolved in CH_3OH–H_2O (50 mL: 50 mL) mixture, compound **3** (50 g, 0.23 mol) added by dripping in 1 h. The mixture was then stirred for 4 h and extracted by chloroform. (2-Trifluoromethylphenyl)-6-[(methylthio) methyl]aniline (**4**, 45 g) was obtained by dried chloroform layer with anhydrous sodium sulfate and removed solvent by rotaryevaporation. Yield 84%.

(2-Trifluoromethylphenyl)-6-(chloromethyl) anilinium chloride (5)

Compound **4** was dissolved in 1,2-dichloroethane and dried gas of hydrogen chloride was added at 50 °C for 50 min. Then, white solid of (2-Trifluoromethylphenyl)-6-(chloromethyl) anilinium chloride (**5**, 42.3 g) was got after the reaction mixture cooled to room temperature. Yield 92%.

(2-Trifluoromethylphenyl)-6-(methyl)aniline (6) and (2-trifluoromethylphenyl)-6-(methoxymethyl)aniline (7)

Compound **5** (42 g, 0.17 mol) were dissolved in 350 mL CH_3OH at room temperature and stirred while 10% Pd–C (14 g), $HCOONH_4$ (322 g, 5.1 mol) were added slowly during 30 min, the reaction mixture was stirred at room temperature overnight before it was filtered through a sintered filter funnel which covered by diatomite. The filtrate was removed CH_3OH by rotaryevaporation and the residue was dissolved in 350 mL H_2O. The pH of the solution was adjusted to 8–9 with 10% NaOH solution. And then the solution was extracted by CH_3COOEt in three times and the ethyl acetate extracts were combined. Compounds **6** and **7** were obtained by dried with anhydrous sodium sulfate, removed solvent by rotaryevaporation and vacuum distillation. Compound **6** was got at the condition of 60–75 °C/20 mm Hg, the yield is 70% and compound **7** was got at the condition of 120–130 °C/20 mm Hg, the yield is 20%, respectively.

N-(2-trifluoromethylphenyl)-6-[(methylthiomethyl) phenyl]-2-chloroacetylamide (8)

Compound **3** (7.0 g, 0.03 mol) and chloroacetic chloride (7.2 mL, 0.09 mol) were dissolved in 50 mL acetonitrile. The reaction mixture was stirred and heated at 50 °C for 3 h and then was removed the acetonitrile. The residue was dissolved in 50 mL dichloromethane, washed with the 10% NaOH solution, dried with anhydrous sodium sulfate and removed solvent by rotaryevaporation. Compound **8** was obtained as a white solid. Yield 72%. Compounds **9**, **12**, **13**, **16**, and **17** were synthesized by the similar procedure in the yields of 68–97%.

General procedure for preparation of the objective compounds

Compound **8** (1.0 g, 0.003 mol), n-propylamine (5.5 mL, 0.067 mol), and K_2CO_3 (0.6 g, 0.004 mol) were added to 10 mL DMF. The mixture was stirred and heated at 40 °C for 10 h and then allowed to cool to room temperature. The excessive n-propylamine was removed by rotaryevaporation and the residue was poured to 100 mL H_2O. The mixture was extracted by CH_3COOEt and the extract was dried with anhydrous sodium sulfate and removed solvent by rotaryevaporation. The residue was dissolved in 50 mL anhydrous ether and dried gas of hydrogen chloride was added at r.t. for 10 min, N-[(2-trifluoromethylphenyl)-6-(methylthiomethyl)phenyl]-2-(1-propylamine)acetylamide hydrochloride (**10a**) was got as a white solid. The other objective compounds were prepared by following the same procedure.

N-[(2-trifluoromethyl-6-methylthiomethyl)phenyl]-2-(1-propylamine) acetylamide hydrochloride (10a)

Yield 79%; mp 99–102 °C; ^{1}H-NMR (500 MHz, CD_3OD) δ 1.03 (3H, t, $J = 7.5$ Hz, 3′-CH_3), 1.77 (2H, m, 2′-CH_2), 2.01 (3H, s, –SCH_3), 3.07 (2H, t, $J = 8.0$ Hz, 1′-NCH_2), 3.72 (2H, m, Ar–CH_2S–), 4.09 (2H, m, 2-$COCH_2$), 7.53 (1H, m, ArH), 7.69 (1H, m, ArH), 7.76 (1H, m, ArH); ^{13}C-NMR (100 MHz, $(CD_3)_2SO$) δ 13.49 (3′-$\underline{C}H_3$), 14.66 (–S$\underline{C}H_3$), 27.23 (2′-$\underline{C}H_2$), 32.70 (Ar–$\underline{C}H_2$S–), 46.46 (1′-N$\underline{C}H_2$), 47.48 (2-CO$\underline{C}H_2$), 121.93 ($\underline{C}$-CF_3), 124.45(Ar), 124.76-127.60 (q, $J = 284$, Ar-$\underline{C}F_3$), 128.80 (Ar), 132.62 (Ar), 134.4 (Ar), 139.58 (Ar), 165.14 (NH$\underline{C}$O). IRν_{max} (KBr, cm^{-1}) 3142, 2968, 1696, 1536, 1469, 1324; ES-MS (*m/z*) $[M + H]^+$: 321; anal. calcd for $C_{14}H_{19}F_3N_2OS.HCl$: C, 47.12; H, 5.65; N, 7.85. Found C, 46.94; H, 5.87; N, 7.74.

N-[(2-trifluoromethyl-6-methylthiomethyl)phenyl]-2-(N,N-diethylamine) acetylamide hydrochloride (10b)

Yield 83%; mp 163–167 °C; ^{1}H-NMR (500 MHz, CD_3OD) δ 1.36 (6H, t, $J = 7.5$ Hz, 2′-CH_3), 1.99 (3H, s, –SCH_3), 3.30 (4H, m, 1′-NCH_2), 3.69 (2H, m, Ar–CH_2S-), 4.20 (2H, m, 2-$COCH_2$), 7.54 (1H, m, ArH), 7.70 (1H, m, ArH), 7.74 (1H, m, ArH); IRν_{max} (KBr, cm^{-1}) 3116, 2982, 1696, 1546, 1469, 1389; ES-MS (*m/z*) $[M + H]^+$: 335; anal. calcd for $C_{15}H_{21}F_3N_2OS.HCl$: C, 48.58; H, 5.98; N, 7.55. Found C, 48.28; H, 5.82; N, 7.59.

N-[(2-trifluoromethyl -6-methylthiomethyl)phenyl]-2-pyrrolidino acetylamide hydrochloride (10c)

Yield 75%; mp 183-185 °C; ^{1}H-NMR (500 MHz, CD_3OD) δ 2.13 (3H, s, –SCH_3), 2.22 (4H, m, 2′-CH_2, 3′-CH_2), 3.30 (2H, m, 1′-NCH, 4′-NCH), 3.82 (2H, m, Ar–CH_2S-), 3.86 (2H, m, 1′-NCH, 4′-NCH), 4.45 (2H, m, 2-$COCH_2$), 7.66 (1H, m, ArH), 7.81 (1H, m, ArH), 7.88 (1H, m, ArH); IRν_{max} (KBr, cm^{-1}) 3490, 2971, 1692, 1535, 1322, 1162; ES-MS (m/z) $[M + H]^+$: 333; anal. calcd for $C_{15}H_{19}F_3N_2OS.HCl$: C, 46.57; H, 5.73; N, 7.24. Found C, 46.43; H, 6.00; N, 7.26.

N-[(2-trifluoromethyl-6-methylthiomethyl)phenyl]-2-piperidino acetylamide hydrochloride (10d)

Yield 97%; mp 92–95 °C; ^{1}H-NMR (500 MHz, CD_3OD) δ 1.60 (2H, m, 2′-CH_2), 1.88 (4H, m, 3′-CH_2, 4′-CH_2), 2.01 (3H, s, –SCH_3), 3.15 (2H, m, 1′-NCH, 5‘-NCH), 3.63 (2H, m, 1′-NCH, 5′-NCH), 3.71 (2H, m, Ar–CH_2S-), 4.21 (2H, m, 2-$COCH_2$), 7.53 (1H, m, ArH), 7.69 (1H, m, ArH), 7.76 (1H, m, ArH); IRν_{max} (KBr, cm^{-1}) 3490, 2971, 1692, 1535, 1322, 1162; ES-MS (*m/z*) $[M + H]^+$: 347; anal. calcd for $C_{16}H_{21}F_3N_2OS.HCl$: C, 47.94; H, 6.03; N, 6.99. Found C, 48.24; H, 6.32; N, 7.10.

N-[(2-trifluoromethyl-6-methylthiomethyl)phenyl]-2-piperidino acetylamide hydrochloride (10e)

Yield 85%; mp 98–101 °C; ^{1}H-NMR (500 MHz, CD_3OD) δ 2.01 (3H, s, –SCH_3), 3.37 (2H, m, 1′-NCH), 3.60 (2H, m, 5′-NCH_2), 3.72 (2H, m, Ar–CH_2S–), 3.85 (2H, m, 2′-OCH_2), 4.05 (2H, m, 4′-OCH_2), 4.32(2H, m, 2-$COCH_2$), 7.54 (1H, m, ArH), 7.70 (1H, m, ArH), 7.76 (1H, m, ArH); IRν_{max} (KBr, cm^{-1}) 3434, 2974, 1693, 1537, 1323, 1164; ES-MS (*m/z*) $[M + H]^+$: 349; anal. calcd for $C_{15}H_{19}F_3N_2O_2S.HCl$: C, 45.74; H, 5.37; N, 7.11. Found C, 45.75; H, 5.66; N, 7.16.

N-[(2-trifluoromethyl-6-methylthiomethyl)phenyl]-2-(1-propylamine) propionamide hydrochloride (11a)

Yield 93%; mp 134–138 °C; ^{1}H-NMR (500 MHz, CD_3OD) δ 1.03 (3H, t, $J = 7.5$ Hz, 3′-CH_3), 1.70 (3H, m, 3-CH_3), 1.79 (2H, m, 2′-CH_2), 2.01 (3H, s, –SCH_3), 3.01 (2H, t, $J =$ 8.0 Hz, 1′-NCH_2), 3.66 (2H, m, Ar–CH_2S-), 4.18 (1H, m, 2-COCH), 7.54 (1H, m, ArH), 7.72 (2H, m, ArH); IRν_{max} (KBr, cm^{-1}) 3121, 2971, 1697, 1538, 1323, 1163; ES-MS (*m/z*) $[M + H]^+$: 335; anal. calcd for $C_{15}H_{21}F_3N_2OS.HCl$: C, 48.50; H, 5.98; N, 7.55. Found C, 48.45; H, 5.99; N, 7.40.

N-[(2-trifluoromethyl-6-methylthiomethyl)phenyl]-2-(N,N-diethylamine) propionamide hydrochloride (11b)

Yield 81%; mp 145-148 °C; ^{1}H-NMR (500 MHz, CD_3OD) δ 1.50 (6H, t, $J = 7.5$ Hz, 2′-CH_3), 1.74 (3H, m, 3-CH_3), 2.02 (3H, s, –SCH_3), 3.40 (4H, m, 1′-NCH_2), 3.66 (2H, m, Ar–CH_2S-), 4.28 (2H, m, 2-$COCH_2$), 7.54 (1H, m, ArH), 7.73 (2H, m, ArH); IRν_{max} (KBr, cm^{-1}) 3146, 2983, 1697, 1529, 1468, 1323; ES-MS (*m/z*) $[M + H]^+$: 349; anal. calcd for $C_{16}H_{23}F_3N_2OS.HCl$: C, 52.10; H, 6.56; N, 7.60. Found C, 52.19; H, 6.56; N, 7.43.

N-[(2-trifluoromethyl-6-methylthiomethyl)phenyl]-2-pyrrolidino propionamide hydrochloride (11c)

Yield 88%; mp 23–25 °C; ^{1}H-NMR (500 MHz, CD_3OD) δ 1.77 (3H, m, 3-CH_3), 2.05 (3H, s, –SCH_3), 2.20 (4H, m, 2′-CH_2, 3′-CH_2), 3.28 (2H, m, 1′-NCH, 4′-NCH), 3.66 (2H, m, Ar–CH_2S–), 3.67 (2H, m, 1′-NCH, 4′-NCH), 4.24 (2H, m, 2-$COCH_2$), 7.51 (1H, m, ArH), 7.72 (2H, m, ArH); IRν_{max} (KBr, cm^{-1}) 3416, 2963, 1693, 1536, 1322, 1163; ES-MS (m/z) $[M + H]^+$: 347; anal. calcd for $C_{16}H_{21}F_3N_2OS.HCl$: C, 50.19; H, 5.79; N, 7.32. Found C, 50.45; H, 6.05; N, 7.34.

N-[(2-trifluoromethyl-6-methylthiomethyl)phenyl]-2-piperidino propionamide hydrochloride (11d)

Yield 79%; mp 185-187 °C; ^{1}H-NMR (500 MHz, CD_3OD) δ 1.60 (2H, m, 2′-CH_2), 1.70 (3H, m, 3-CH_3), 1.88 (4H, m, 3′-CH_2, 4′-CH_2), 2.02 (3H, s, –SCH_3), 3.08 (2H, m, 1′-NCH, 5‘-NCH), 3.63 (2H, m, 1′-NCH, 5‘-NCH), 3.70 (2H, m, Ar–CH_2S–), 4.20 (2H, m, 2-$COCH_2$), 7.55 (1H, m, ArH), 7.73 (2H, m, ArH); IRν_{max} (KBr, cm^{-1}) 3111, 2980, 1692, 2543, 1702, 1532; ES-MS (m/z) $[M + H]^+$: 362; anal. calcd for $C_{17}H_{23}F_3N_2OS.HCl$: C, 49.94; H, 6.28; N, 7.28. Found C, 49.67; H, 6.58; N, 7.06.

N-[(2-trifluoromethyl-6-methylthiomethyl)phenyl]-2-piperidino propionamide hydrochloride (11e)

Yield 85%; mp 92-95 °C; ^{1}H-NMR (500 MHz, CD_3OD) δ 1.77 (3H, m, 3-CH_3), 2.02 (3H, s, –SCH_3), 3.30 (2H, m, Ar–CH_2S-), 3.45(2H, m, 1′-NCH_2), 3.49 (2H, m, 5′-NCH_2), 3.96 (2H, m, 2′-OCH_2), 4.06 (2H, m, 4′-OCH_2), 4.26(2H, m, 2-$COCH_2$), 7.54 (1H, m, ArH), 7.73 (2H, m, ArH); IRν_{max} (KBr, cm^{-1}) 3147, 2971, 1693, 1533, 1322, 1162; ES-MS (*m/z*) $[M+H]^+$: 363; anal. calcd for $C_{16}H_{21}F_3N_2O_2S$.HCl: C, 46.10; H, 5.80; N, 6.72. Found C, 46.36; H, 6.07; N, 6.71.

N-[(2-trifluoromethyl-6-methyl)phenyl]-2-(1-propylamine) acetylamide hydrochloride (14a)

Yield 81%; mp 225-228 °C; ^{1}H-NMR (500 MHz, CD_3OD) δ 1.03 (3H, t, $J = 7.5$ Hz, 3′-CH_3), 1.76 (2H, m, 2′-CH_2),2.35(3H, s, $ArCH_3$), 3.05 (2H, m, 1′-NCH_2), 4.08 (2H, m, 2-$COCH_2$), 7.40 (1H, m, ArH), 7.59 (2H, m, ArH); IRν_{max} (KBr, cm^{-1}) 3262, 2954, 2772, 1682, 1537, 1324, 1161; ES-MS (*m/z*) $[M+H]^+$: 275; anal. calcd for $C_{13}H_{17}F_3N_2O$.HCl: C, 50.25; H, 5.84; N, 9.01. Found C, 50.31; H, 5.99; N, 9.01.

N-[(2-trifluoromethyl-6-methyl)phenyl]-2-(N,N-diethylamine) acetylamide hydrochloride (14b)

Yield 77%; mp 170–172 °C; ^{1}H-NMR (500 MHz, CD_3OD) δ 1.37 (6H, t, $J = 7.2$ Hz, 2′-CH_3), 2.29 (3H, s, –CH_3), 3.35 (4H, m, 1′-NCH_2), 4.25 (2H, m, 2-$COCH_2$), 7.45 (1H, m, ArH), 7.60 (2H, m, ArH); IRν_{max} (KBr, cm^{-1}) 3459, 3123, 2983, 1691, 1537, 1472, 1323; ES-MS (*m/z*) $[M+H]^+$: 289; anal. calcd for $C_{14}H_{19}F_3N_2O$.HCl: C, 50.38; H, 6.34; N, 8.39. Found C, 50.34; H, 6.60; N, 8.51.

N-[(2-trifluoromethyl-6-methyl)phenyl]-2-pyrrolidino acetylamide hydrochloride (14c)

Yield 75%; mp 183–185 °C; ^{1}H-NMR (500 MHz, CD_3OD) δ 2.03 (2H, m, 2′-CH_2), 2.20 (2H, m, 3′-CH_2), 2.29(3H, s, $ArCH_3$), 3.18(2H, m, 1′-NCH, 4′-NCH), 3.75 (2H, m, 1′-NCH, 4′-NCH), 4.35 (2H, m, 2-$COCH_2$), 7.45 (1H, m, ArH), 7.59 (2H, m, ArH); IRν_{max} (KBr, cm^{-1}) 3419, 2948, 1692, 1599, 1471, 1323; ES-MS (*m/z*) $[M+H]^+$: 287; anal. calcd for $C_{14}H_{17}F_3N_2O$.HCl: C, 50.38; H, 5.73; N, 8.39. Found C, 50.34; H, 5.72; N, 8.49.

N-[(2-trifluoromethyl-6-methyl)phenyl]-2-piperidino acetylamide hydrochloride (14d)

Yield 74%; mp 173–175 °C; ^{1}H-NMR (500 MHz, CD_3OD) δ 1.60 (2H, m, 2′-CH_2), 2.28 (4H, m, 3‘-CH_2, 4′-CH_2), 2.42 (3H, s, –$ArCH_3$), 3.26 (2H, m, 1′-NCH, 5′-NCH), 3.73 (2H, m, 1′-NCH, 5′-NCH), 4.30 (2H, m, 2-$COCH_2$), 7.59 (1H, m, ArH), 7.73 (2H, m, ArH); IRν_{max} (KBr, cm^{-1}) 3382, 1690, 1575, 1544, 1472, 1323; ES-MS (*m/z*) $[M+H]^+$: 301; anal. calcd for $C_{15}H_{19}F_3N_2O$.HCl: C, 50.78; H, 6.25; N, 7.90. Found C, 50.67; H, 6.27; N, 7.84.

N-[(2-trifluoromethyl-6-methyl)phenyl]-2-piperidino acetylamide hydrochloride (14e)

Yield 74%; mp 115–118 °C; ^{1}H-NMR (500 MHz, CD_3OD) δ 2.30 (3H, s, –$ArCH_3$), 3.33 (2H, m, 1′-NCH), 3.47 (2H, m, 5′-NCH_2), 3.87 (2H, m, 2′-OCH_2), 4.04 (2H, m, 4′-OCH_2), 4.29 (2H, m, 2-$COCH_2$), 7.75 (1H, m, ArH), 7.60 (2H, m, ArH); IRν_{max} (KBr, cm^{-1}) 3438, 2977, 1692, 1536, 1323, 1164; ES-MS (m/z) $[M+H]^+$: 303; anal. calcd for $C_{14}H_{17}F_3N_2O_2$.HCl: C, 47.13; H, 5.65; N, 7.85. Found C, 47.43; H, 5.93; N, 7.89.

N-[(2-trifluoromethyl-6-methyl)phenyl]-2-(1-propylamine) propionamide hydrochloride (15a)

Yield 92%; mp 115–118 °C; ^{1}H-NMR (500 MHz, CD_3OD) δ 1.03 (3H, t, $J = 7.2$ Hz, 3′-CH_3), 1.70 (3H, m, 3-CH_3), 1.79 (2H, m, 2′-CH_2), 2.29 (3H, m, Ar–CH_3), 2.97 (2H, m, 1′-NCH_2), 4.18 (1H, m, 2-COCH), 7.44 (1H, m, ArH), 7.61 (2H, m, ArH); IRν_{max} (KBr, cm^{-1}) 3533, 3194, 2978, 1697, 1557, 1550, 1323, 1165; ES-MS (*m/z*) $[M+H]^+$: 289; anal. calcd for $C_{14}H_{19}F_3N_2O$.HCl: C, 51.78; H, 6.21; N, 8.63. Found C, 51.67; H, 6.34; N, 8.49.

N-[(2-trifluoromethyl-6-methyl)phenyl]-2-(N,N-diethylamine) propionamide hydrochloride (15b)

Yield 80%; mp 205-207 °C; ^{1}H-NMR (500 MHz, CD_3OD) δ 1.50 (6H, m, 2′-CH_3), 1.86 (3H, m, 3-CH_3), 2.42 (3H, s, Ar–CH_3), 3.45(4H, m, 1′-NCH_2), 4.45 (1H, m, 2-COCH), 7.59 (1H, m, ArH), 7.74 (2H, m, ArH); IRν_{max} (KBr, cm^{-1}) 3170, 2985, 1695, 1527, 1325; ES-MS (*m/z*) $[M+H]^+$: 303; anal. calcd for $C_{15}H_{21}F_3N_2O$.HCl: C, 53.18; H, 6.55; N, 8.27. Found C, 52.96; H, 6.64; N, 8.00.

N-[(2-trifluoromethyl-6-methyl)phenyl]-2-pyrrolidino propionamide hydrochloride (15c)

Yield 75%; mp 220-221 °C; ^{1}H-NMR (500 MHz, CD_3OD) δ 1.73 (3H, d, $J = 17.5$ Hz, 3-CH_3), 2.18 (4H, m, 2′-CH_2, 3′-CH_2), 2.29 (3H, d, $J = 16$ Hz, Ar–CH_3), 3.29 (2H, 1′-NCH, 4′-NCH), 3.67 (2H, m, 1′-NCH, 4′-NCH), 4.25 (1H, m, 2-COCH), 7.46 (1H, m, ArH), 7.60 (2H, m, ArH); IRν_{max} (KBr, cm^{-1}) 3458, 2963, 1690, 1686, 1543, 1323, 1165; ES-MS (*m/z*) $[M+H]^+$: 301; anal. calcd for $C_{15}H_{19}F_3N_2O$.HCl.1/2H_2O: C, 52.10; H, 6.12; N, 8.10. Found C, 51.98; H, 6.36; N, 8.01.

N-[(2-trifluoromethyl-6-methyl)phenyl]-2-piperidino propionamide hydrochloride (15d)

Yield 78%; mp 98–101 °C; ^{1}H-NMR (500 MHz, CD_3OD) δ 1.50 (2H, m, 2′-CH_2), 1.60 (3H, m, 3-CH_3), 1.80 (4H, m, 3′-CH_2, 4′-CH_2), 2.29 (3H, d, $J = 11$ Hz, Ar–CH_3), 3.12 (2H, m, 1′-NCH, 5′-NCH), 3.63 (2H, m, 1′-NCH, 5′-NCH), 4.25 (1H, m, 2-COCH), 7.46 (1H, m, ArH), 7.60 (2H, m, ArH); IRν_{max} (KBr, cm^{-1}) 3438, 2953, 1692, 1536, 1471, 1322; ES-MS (m/z) $[M + H]^+$: 315; anal. calcd for $C_{16}H_{21}F_3N_2O.HCl.H_2O$: C, 52.10; H, 6.56; N, 7.60. Found C, 51.92; H, 6.61; N, 7.53.

N-[(2-trifluoromethyl-6-methyl)phenyl]-2-piperidino propionamide hydrochloride (15e)

Yield 85%; mp 126–128 °C; ^{1}H-NMR (500 MHz, CD_3OD) δ 1.46 (3H, d, $J = 6.9$ Hz, 3-CH_3), 2.30 (3H, m, Ar–CH_3), 3.46 (2H, m, 2′-NCH_2), 3.52 (2H, m, 5′-NCH_2), 4.06 (2H, m, 3′-OCH_2), 4.11 (1H, m, 4′-OCH_2), 4.21(1H, m, 2-COCH), 7.48 (1H, m, ArH), 7.62 (2H, m, ArH); IRν_{max} (KBr, cm^{-1}) 3444, 2972, 1692, 1536, 1323, 1165; ES-MS (*m/z*) $[M + H]^+$: 317; anal. calcd for $C_{15}H_{19}F_3N_2O_2.HCl.H_2O$: C, 48.59; H, 5.98; N, 7.55. Found C, 48.79; H, 6.29; N, 7.56.

N-[(2-trifluoromethyl-6-methylxymethyl)phenyl]-2-(1-propylamine) acetylamide hydrochloride (18a)

Yield 82%; mp 167–170 °C; ^{1}H-NMR (500 MHz, CD_3OD) δ 1.03 (3H, t, $J = 7.5$ Hz, 3′-CH_3), 1.76 (2H, m, 2′-CH_2), 3.05 (2H, t, $J = 8.0$ Hz, 1′-NCH_2), 3.30 (3H, s, –OCH_3), 4.06 (2H, m, 2-$COCH_2$), 4.46 (2H, s, Ar–CH_2O–), 7.56 (1H, m, ArH), 7.72 (1H, m, ArH), 7.78 (1H, m, ArH); IRν_{max} (KBr, cm^{-1}) 3269, 2943, 2886, 1681, 1542, 1325; ES-MS (*m/z*) $[M + H]^+$: 305; anal. calcd for $C_{14}H_{19}F_3N_2O_2.HCl$: C, 46.87; H, 6.17; N, 7.81. Found C, 47.13; H, 6.17; N, 7.89.

N-[(2-trifluoromethyl-6-methylxymethyl)phenyl]-2- (N,N-diethylamine) acetylamide hydrochloride (18b)

Yield 80%; mp 165–168 °C; ^{1}H-NMR (500 MHz, CD_3OD) δ 1.37 (6H, t, $J = 7.2$ Hz, 2′-CH_3), 3.30 (3H, s, –OCH_3), 3.36 (4H, m, 1′-NCH_2), 4.20 (2H, m, Ar–CH_2O-), 4.47 (2H, s, 2-$COCH_2$), 7.59 (1H, m, ArH), 7.77 (2H, m, ArH); IRν_{max} (KBr, cm^{-1}) 3519, 2947, 1688, 1538, 1467, 1391; ES-MS (*m/z*) $[M + H]^+$: 319; anal. calcd for $C_{15}H_{21}F_3N_2O_2.HCl$: C, 50.78; H, 6.25; N, 7.90. Found C, 50.75; H, 6.40; N, 7.70.

N-[(2-trifluoromethyl-6-methylxymethyl)phenyl]-2-pyrrolidino acetylamide hydrochloride (18c)

Yield 72%; mp 205–208 °C; ^{1}H-NMR (500 MHz, CD_3OD) δ 2.10 (4H, m, 2′-CH_2, 3‘-CH_2), 3.18 (2H, m, 1′-NCH, 4′-NCH), 3.38 (3H, s, –OCH_3), 3.77 (2H, m, 1′-NCH, 4‘-NCH), 4.34 (2H, m, 2-$COCH_2$), 4.47 (2H, s, Ar–CH_2O), 7.57 (1H, m, ArH), 7.74 (1H, m, ArH), 7.79 (1H, m, ArH); IRν_{max} (KBr, cm^{-1}) 3471, 2977, 1692, 1536, 1323; ES-MS (m/z) $[M + H]^+$: 317; anal. calcd for $C_{15}H_{19}F_3N_2O_2.HCl$: C, 51.07; H, 5.71; N, 7.94. Found C, 51.57; H, 5.87; N, 7.98.

N-[(2-trifluoromethyl-6-methylxymethyl)phenyl]-2-piperidino acetylamide hydrochloride (18d)

Yield 77%; mp 157–159 °C; ^{1}H-NMR (500 MHz, CD_3OD) δ 1.60 (2H, m, 2′-CH_2), 1.88 (4H, m, 3′-CH_2, 4′-CH_2), 3.15 (2H, m, 1′-NCH, 5′-NCH), 3.37 (3H, s, –OCH_3), 3.61(2H, m, 1′-NCH, 5′-NCH), 4.20 (2H, m, 2-$COCH_2$), 4.47 (2H, m, Ar–CH_2O–), 7.58 (1H, m, ArH), 7.73 (1H, m, ArH), 7.79 (1H, m, ArH); IRν_{max} (KBr, cm^{-1}) 3119, 2950, 1686, 1539, 1469, 1322, 1163; ES-MS (*m/z*) $[M + H]^+$: 331; anal. calcd for $C_{16}H_{21}F_3N_2O_2.HCl$: C, 52.39; H, 6.05; N, 7.64. Found C, 52.46; H, 5.99; N, 7.68.

N-[(2-trifluoromethyl-6-methylxymethyl)phenyl]-2-piperidino acetylamide hydrochloride (18e)

Yield 81%; mp 101–103 °C; ^{1}H-NMR (500 MHz, CD_3OD) δ 3.30 (3H, s, –OCH_3), 3.33 (2H, m, 1′-NCH), 3.57 (2H, m, 5′-NCH_2), 3.89 (2H, m, 2′-OCH_2), 4.05 (2H, m, Ar–CH_2O-), 4.30 (2H, m, 2-OCH_2), 4.47(2H, m, 4′-CH_2O), 7.57 (1H, m, ArH), 7.71 (1H, m, ArH), 7.78 (1H, m, ArH); IRν_{max} (KBr, cm^{-1}) 3414, 1685, 1325, 1166, 1125; ES-MS (*m/z*) $[M + H]^+$: 333; anal. calcd for $C_{15}H_{19}F_3N_2O_3.HCl.H_2O$: C, 46.58; H, 5.73; N, 7.24. Found C, 46.83; H, 5.99; N, 7.37.

N-[(2-trifluoromethyl-6-methylxymethyl)phenyl]-2-(1-propylamine) propionamide hydrochloride (19a)

Yield 96%; mp 96–98 °C; ^{1}H-NMR (500 MHz, CD_3OD) δ 1.03 (3H, t, $J = 7.5$ Hz, 3′-CH_3), 1.70 (3H, d, $J = 6.6$ Hz, 3-CH_3), 1.80 (2H, m, 2′-CH_2), 3.00 (2H, D, $J = 6.6$ Hz, 1′-NCH_2), 3.30 (3H, s, –OCH_3), 4.17 (1H, m, 2-COCH), 4.45 (2H, s, Ar–CH_2O-), 7.58 (1H, m, ArH), 7.77 (2H, m, ArH); IRν_{max} (KBr, cm^{-1}) 3152, 2975, 1702, 1536, 1465, 1326, 1163; ES-MS (*m/z*) $[M + H]^+$: 319; anal. calcd for $C_{15}H_{21}F_3N_2O_2.HCl$: C, 50.78; H, 6.25; N, 7.90. Found C, 50.68; H, 6.40; N, 7.76.

N-[(2-trifluoromethyl-6-methylxymethyl)phenyl]-2-(N,N-diethylamine) propionamide hydrochloride (19b)

Yield 84%; mp 121–123 °C; ^{1}H-NMR (500 MHz, CD_3OD) δ 1.36 (6H, d, $J = 7.5$ Hz, 2′-CH_3), 1.72 (3H, m, 3-CH_3), 3.30 (3H, s, –OCH_3), 3.33 (4H, m, 1′-NCH_2), 4.27 (1H, m, 2-COCH), 4.47(2H, s, Ar–CH_2O–), 7.59 (1H, m, ArH), 7.77 (2H, m, ArH); IRν_{max} (KBr, cm^{-1}) 3147, 2983, 1693, 1527, 1324, 1162; ES-MS (*m/z*) $[M + H]^+$: 333; anal. calcd for $C_{16}H_{23}F_3N_2O_2$.HCl: C, 50.78; H, 6.25; N, 7.90. Found C, 50.88; H, 6.25; N, 7.69.

N-[(2-trifluoromethyl-6-methylxymethyl)phenyl]-2-pyrrolidino propionamide hydrochloride (19c)

Yield 81%; mp 218–220 °C; ^{1}H-NMR (500 MHz, CD_3OD) δ 1.73 (3H, m, 3-CH_3), 2.20 (4H, m, 2′-CH_2, 3′-CH_2), 3.29 (2H, m, 1′-NCH, 4′-NCH), 3.34 (3H, s, –OCH_3), 3.67 (2H, m, 1′-NCH, 4′-NCH), 4.34 (1H, m, 2-COCH), 4.47 (2H, d, $J = 11.5$ Hz, Ar–CH_2O-), 7.57 (1H, m, ArH), 7.76 (2H, m, ArH); IRν_{max} (KBr, cm^{-1}) 3110, 2951, 1685, 1535, 1321, 1163; ES-MS (m/z) $[M + H]^+$: 331; anal. calcd for $C_{16}H_{21}F_3N_2O_2$.HCl: C, 52.39; H, 6.05; N, 7.64. Found C, 52.10; H, 6.32; N, 7.65.

N-[(2-trifluoromethyl-6-methylxymethyl)phenyl]-2-piperidino propionamide hydrochloride (19d)

Yield 74%; mp 180–183 °C; ^{1}H-NMR (500 MHz, CD_3OD) δ 1.60 (2H, m, 2′-CH_2), 1.70 (3H, m, 3-CH_3), 1.88 (4H, m, 3′-CH_2, 4′-CH_2), 3.09 (2H, m, 1′-NCH, 5′-NCH), 3.30 (3H, s, –OCH_3), 3.64 (2H, m, 1′-NCH, 5′-NCH), 4.18 (1H, m, 2-COCH), 4.48(2H, m, Ar–CH_2O-), 7.58 (1H, m, ArH), 7.77 (2H, m, ArH); IRν_{max} (KBr, cm^{-1}) 3092, 2939, 1690, 1532, 1466, 1386, 1319, 1161; ES-MS (*m/z*) $[M + H]^+$: 345; anal. calcd for $C_{17}H_{23}F_3N_2O_2$.HCl: C, 53.61; H, 6.35; N, 7.36. Found C, 53.57; H, 6.57; N, 7.45.

N-[(2-trifluoromethyl-6-methylxymethyl)phenyl]-2-piperidino propionamide hydrochloride (19e)

Yield 79%; mp 235–238 °C; ^{1}H-NMR (500 MHz, CD_3OD) δ 1.76 (3H, d, $J = 6.6$ Hz, 3-CH_3), 3.36 (3H, s, –OCH_3), 3.39 (2H, m, 1′-NCH_2), 3.41 (2H, m, 5′-NCH_2), 3.82 (2H, m, 2′-OCH_2), 4.08(2H, M, Ar–CH_2O-), 4.27(1H, m, 2-COCH), 4.53 (2H, m, 4′-OCH_2), 7.60 (1H, m, ArH), 7.77 (2H, m, ArH); IRν_{max} (KBr, cm^{-1}) 3100, 2943, 1688, 1532, 1320, 1165; ES-MS (*m/z*) $[M + H]^+$: 347; anal. calcd for $C_{16}H_{21}F_3N_2O_3$.HCl: C, 50.20; H, 5.79; N, 7.32. Found C, 50.20; H, 6.04; N, 7.31.

Biological evaluation

The sciatic nerve block activities in toads of the objective compounds were determined as previously described (Li et al. 2017). Electrophysiological experimental data were obtained on Doctor-95 Super Lab (Jiangsu Medicine technological institute). All the experiments were tested with the isolated sciatic nerves of wild adult toads. Lidocaine was got from Shanghai Xidi Biotech. Co., Ltd and was tested after dissolving in Ringer's solutions. Record the experimental data. The regress equation of AP decreasing extent (%) and compounds concentration was $y = \text{blog}x + a$ (y: AP decreasing extent (%); x: drug concentration; a, b: regress coefficient). The regress equation of latent period and compounds concentration was $y = \text{blog}x + \text{a}$ (y: latent period; x: drug concentration; a, b: regress coefficient). The ED_{50} and latent time were calculated by those equations.

Molecular docking studies

In this research, the crystal structures of VGSC (PDB code: 6AGF), GABAA-R (PDB code: 6D1S), and NMDA-R (PDB code: 5I2N) were obtained from RSCB Protein Data Bank, and the docking studies were performed on the software program MOE 2015.10. The preparation of the docking study has two parts, the pretreatment of receptor proteins and ligands. Firstly, under Amber 10: EHT force field, these protein structures are processed using the default parameters of the Quickprep module: adding hydrogen atoms, removing water, and repairing missing residues. After pretreatment, the protonation state of the residues was determined under the condition of pH = 7. Next, the three-dimensional structures of compounds **10a**, **14e,** and lidocaine were constructed under Amber 10: EHT force field and the conformational database of structures were provided for further docking study by energy minimization and conformation search. Finally, all conformations were docked into the binding sites of three different receptor proteins using the Induced Fit protocol under default parameters, and the amino acid residues within 6 Å of the ligand, and ligands were set to be flexible. The docking poses were obtained by the Triangle Matcher method and scored by GBVI/WSA dG. And the docking results held 20 docking postures per ligand with default parameters for further visual analysis.

Conclusion

In this paper, we presented the synthesis, sciatic nerve block activities, dissociation constants and molecular docking

results of fluoro-substituted lidocaine analogs. Twelve of compounds displayed significant potency higher than or similar to that of the reference compound lidocaine. Twenty-five of these compounds had shorter latent periods than that of lidocaine. Fifteen of them showed pKa values of 7.5–7.8 suitable for local anesthesia. Among these, **10a** was the most favorable analog proving the highest potency, relatively short latent periods and suitable pKa. The molecular docking results identified the hydrophobic interactions and hydrogen bonding formed by compounds **10a** and lidocaine and receptor proteins VGSC, GABAA-R and NMDA-R, which may be crucial in optimization and prediction of the sciatic nerve block activities of the lidocaine analogs in local anesthesia. Most importantly, this work verified our initial proposition that substitution with a trifluoromethyl group at the benzene ring of lidocaine could induce higher local anesthetic activity and shorter latent periods.

Acknowledgements This work was supported by a grant from Jiangsu Hengrui Pharmaceutical Com. Ltd and a foundation on the integration of industry, education, and research of He'nan science and technology commission (No. 152107000041). The authors are grateful to Dr J.H. Fu (Pharmaceutical School, China Pharmaceutical University) for the determination of biological activity. We thank Amy Tong from Liwen Bianji, Edanz Editing China (www.liwenbianji.cn/ac), for editing the English draft of this paper.

Compliance with ethical standards

Conflict of interest The authors declare that they have no conflict of interest.

References

Adler DMT, Damborg P, Verwilghen DR (2017) The antimicrobial activity of bupivacaine, lidocaine and mepivacaine against equine pathogens: an investigation of 40 bacterial isolates. Vet J 223:27–31

Amin J, Subbarayan MS (2017) Orthosteric- versus allosteric-dependent activation of the GABAA receptor requires numerically distinct subunit level rearrangements. Sci Rep 7:7770

Bonniaud P, Camus P (2015) Rare and emergent drug-induced and iatrogenic respiratory conditions: a guide to their recognition and management. Orphan Lung Dis:541–580

Boukhabza M, El Hilaly J, Attiya N, El-Haidani A, Filali-Zegzouti Y, Mazouzi D, Amarouch MY (2016) In silico evaluation of the potential antiarrhythmic effect of epigallocatechin-3-gallate on cardiac channelopathies. Comput Math Methods Med 2016:7861653

Chen LL, Zhang S, Q YM (2011) Effect of MK-801 on seizure induced by lidocaine in Rats. J Clin Anesth 27:812–814

Chen Q, Wells MM, Arjunan P, Tillman TS, Cohen AE, Xu Y, Tang P (2018) Structural basis of neurosteroid anesthetic action on GABAA receptors. Nat Commun 9:3972

D'Agostino G, Saporito A, Cecchinato V, Silvestri Y, Borgeat A, Anselmi L, Uguccioni M (2018) Lidocaine inhibits cytoskeletal remodelling and human breast cancer cell migration. Br J Anaesth 121:962–968

Epstein E (1998) Antimicrobial effects of lidocaine, bicarbonate, and epinephrine. J Am Acad Dermatol 39:518–519

Estebe JP (2017) Intravenous lidocaine. Best Pract Res Clin Anaesthesiol 31:513–521

Gronwald C, Vegh V, Hollmann MW, Hahnenkamp A, Garaj V, Hahnenkamp K (2012) The inhibitory potency of local anesthetics on NMDA receptor signalling depends on their structural features. Eur J Pharm 674:13–19

Hebbes C, Thompson JP (2018) Drugs acting on the heart: antiarrhythmics. Anaesth Intensive Care Med 19:370–374

Kan H, Wang Y, Wang D, Sun H, Zhou S, Wang H, Guan J, Li M (2018) Cordycepin rescues lidocaine-induced neurotoxicity in dorsal root ganglion by interacting with inflammatory signaling pathway MMP3. Eur J Pharm 827:88–93

Kyburz E, Spiegelberg H, (1975) Tricyclic amines and processes for the preparation thereof. Patent No. US3884967

Le Gac G, Angenard G, Clement B, Laviolle B, Coulouarn C, Beloeil H (2017) Local anesthetics inhibit the growth of human hepatocellular carcinoma cells. Anesth Analg 125:1600–1609

Li J, Wang G, Xu W, Ding M, Yu W (2018) Efficacy of intravenous lidocaine on pain relief in patients undergoing laparoscopic cholecystectomy: a meta-analysis from randomized controlled trials. Int J Surg 50:137–145

Li W, Ding L, Liu H-M, You Q (2017) Synthesis, biological evaluation, and molecular docking of ropivacaine analogs as local anesthetic agents. Med Chem Res 27:954–965

Li W, Xiao B, Zhou Y, Liu HM (2010) Synthesis and analgetic activity of imipramine analoges. Chin J Org Chem 30:898–903

Li W, You Q (2007) Synthesis and local anesthetic activity of fluoro-substituted imipramine and its analogues. Bioorg Med Chem Lett 17:3733–3735

Lin D, Cao L, Wang Z, Li J, Washington JM, Zuo Z (2012) Lidocaine attenuates cognitive impairment after isoflurane anesthesia in old rats. Behav Brain Res 228:319–327

Lipkind GM, Fozzard HA (2010) Molecular model of anticonvulsant drug binding to the voltage-gated sodium channel inner pore. Mol Pharmacol 78:631–638

J. e Silva LO, Scherber K, Cabrera D, Motov S, J. Erwin P, P. West C, Murad MH, Bellolio MF (2018) Safety and efficacy of intravenous lidocaine for pain management in the emergency department: a systematic review. Ann Emerg Med 72:135–144 e133

McLeod SL, Brignardello-Petersen R, Worster A, You J, Iansavichene A, Guyatt G, Cheskes S (2017) Comparative effectiveness of antiarrhythmics for out-of-hospital cardiac arrest: A systematic review and network meta-analysis. Resuscitation 121:90–97

Nakahata Y, Miyamoto A, Watanabe M, Moorhouse AJ, Nabekura J, Ishibashi H (2010) Depolarizing shift in the GABA-induced current reversal potential by lidocaine hydrochloride. Brain Res 1345:19–27

Neuwersch S, Köstenberger M, Sorschag S, Ilias W, Likar R (2017) Antimicrobial activity of lidocaine, bupivacaine, mepivacaine and ropivacaine on *Staphylococcus epidermidis, Staphylococcus aureus* and *Bacillus subtilis*. Open Pain J 10:1–4

Ojima I (2004) Use of fluorine in the medicinal chemistry and chemical biology of bioactive compounds-a case study on fluorinated taxane anticancer agents. Chembiochem 5:628–635

Pan X, Li Z, Zhou Q, Shen H, Wu K, Huang X, Chen J, Zhang J, Zhu X, Lei J, Xiong W, Gong H, Xiao B, Yan N (2018) Structure of the human voltage-gated sodium channel Nav1.4 in complex with beta1. Science 362

Strother A, Soong SL, Dev V, Sadri M (1977) Structure activity relationship of lidocaine type local anesthetics. Life Sci 21:71–81

Sugimoto M, Uchida I, Fukami S, Takenoshita M, Mashimo T, Yoshiya I (2000) The alpha and gamma subunit-dependent effects of local anesthetics on recombinant GABA(A) receptors. pdf. Eur J Pharm 401:329–337

Tavare AN, Perry NJ, Benzonana LL, Takata M, Ma D (2012) Cancer recurrence after surgery: direct and indirect effects of anesthetic agents. Int J Cancer 130:1237–1250

Tulgar S, Alasehir EA, Selvi O (2018) The antimicrobial activity of ephedrine and admixture of ephedrine and propofol: an in vitro study. Braz J Anesth 68:69–74

Van Ness M, Jensen H, Adamson GN, Kysar PE, Holland P (2013) Neutrophils contain cholesterol crystals in transfusion-related acute lung injury (TRALI). Am J Clin Pathol 140:170–176

Volgraf M, Sellers BD, Jiang Y, Wu G, Ly CQ, Villemure E, Pastor RM, Yuen PW, Lu A, Luo X, Liu M, Zhang S, Sun L, Fu Y, Lupardus PJ, Wallweber HJ, Liederer BM, Deshmukh G, Plise E, Tay S, Reynen P, Herrington J, Gustafson A, Liu Y, Dirksen A, Dietz MG, Liu Y, Wang TM, Hanson JE, Hackos D, Scearce-Levie K, Schwarz JB (2016) Discovery of GluN2A-selective NMDA receptor positive allosteric modulators (PAMs): tuning deactivation kinetics via structure-based design. J Med Chem 59:2760–2779

Wang HW, Wang LY, Jiang L, Tian SM, Zhong TD, Fang XM (2016) Amide-linked local anesthetics induce apoptosis in human non-small cell lung cancer. J Thorac Dis 8:2748–2757

Wang J, Liu H (2011) Application of fluorine in drug design. Chin J Org Chem 31:1785–1798

Wang L, Wang M, Li S, Wu H, Shen Q, Zhang S, Fang L, Liu R (2018) Nebulized lidocaine ameliorates allergic airway inflammation via downregulation of TLR2. Mol Immunol 97:94–100

Wang L, Zellmer SG, Printzenhoff DM, Castle NA (2015) Addition of a single methyl group to a small molecule sodium channel inhibitor introduces a new mode of gating modulation. Br J Pharmacol 172:4905–4918

Yang S, Gu C, Mandeville ET, Dong Y, Esposito E, Zhang Y, Yang G, Shen Y, Fu X, Lo EH, Xie Z (2017) Anesthesia and surgery impair blood-brain barrier and cognitive function in mice. Front Immunol 8:902

Ye JH, Ren J, Krnjevic K, Liu PL, Mcardle JJ (1999) Cocaine and lidocaine have additive inhibitory effects on the GABA current A of acutely dissociated hippocampal pyramidal neurons. Brain Res 821:26–32

Zhang L, Tanabe K, Yanagidate F, Kawasaki Y, Chen G, Dohi S, Iida H (2014) Different effects of local anesthetics on extracellular signal-regulated kinase phosphorylation in rat dorsal horn neurons. Eur J Pharmacol 734:132–136